Electronic Supplementary Information (ESI)

Surface Structure Evolution of Bimetallic Nickel Tungsten Nitride (Ni_2W_3N) for High Performance Hydrogen Evolution

Ji Young Hwang[a], Yeonju Park[b], Young Mee Jung[*b], Hyung-Kyu Lim[*a], Duck Hyun Youn[*a]

[a] *Department of Chemical Engineering, Department of Integrative Engineering for Hydrogen Safety, Kangwon National University, Chuncheon 24341, South Korea.*

[b]*Department of Chemistry, Institution for Molecular Science and Fusion Technology, Kangwon Radiation Convergence Research Support Center, Kangwon National University, Chuncheon, 24341, South Korea*

*Corresponding authors

E-mail address: ymjung@kangwon.ac.kr (Y.M.J), hklim@kangwon.ac.kr (H.-K.L.), youndh@kangwon.ac.kr (D.H.Y.)

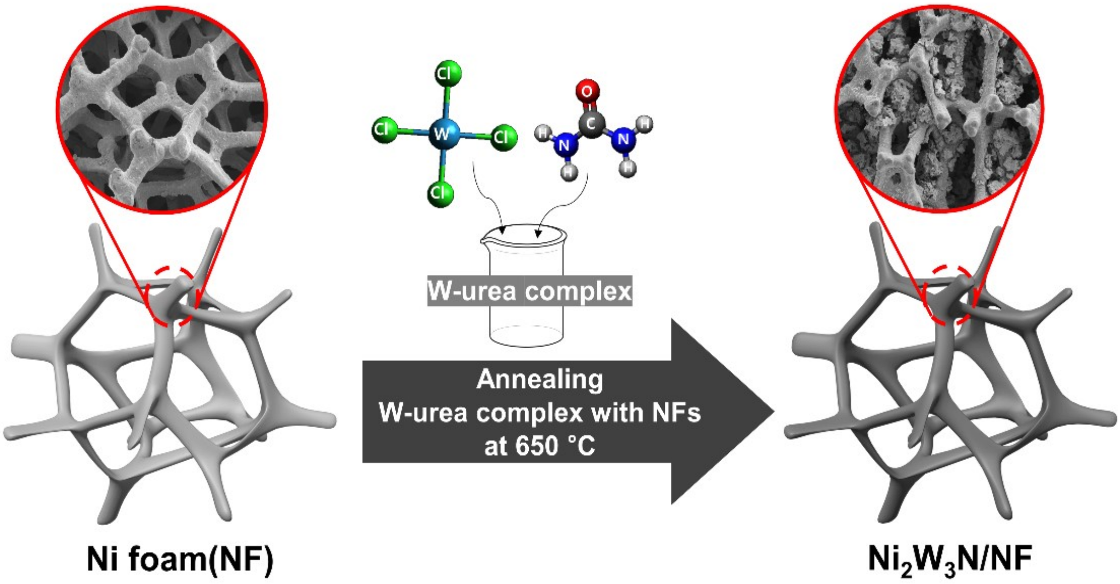

Fig. S1. Schematic illustration for synthetic method of Ni_2W_3N/NF.

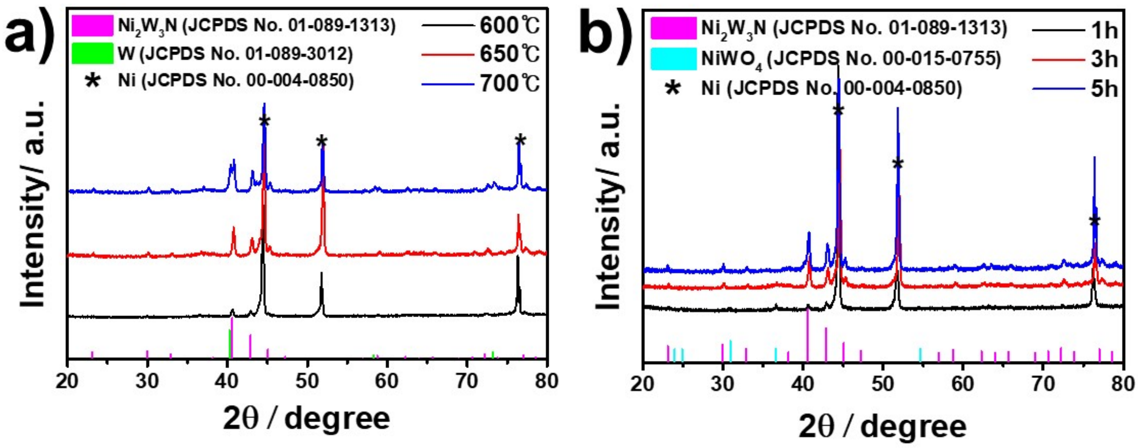

Fig. S2. XRD patterns of the prepared samples a) at different annealing temperatures (fixed duration: 3h) and b) at different annealing durations (fixed temperature: 650 °C).

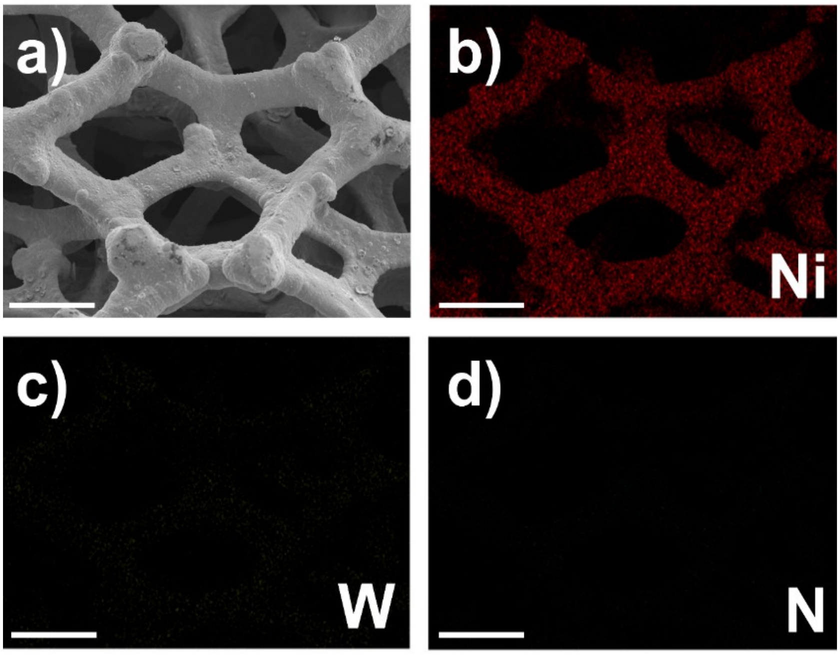

Fig. S3. (a) SEM images of NF and corresponding EDS mapping images of (b) Ni, (c) W, (d) N. Scale bars denote 200 um.

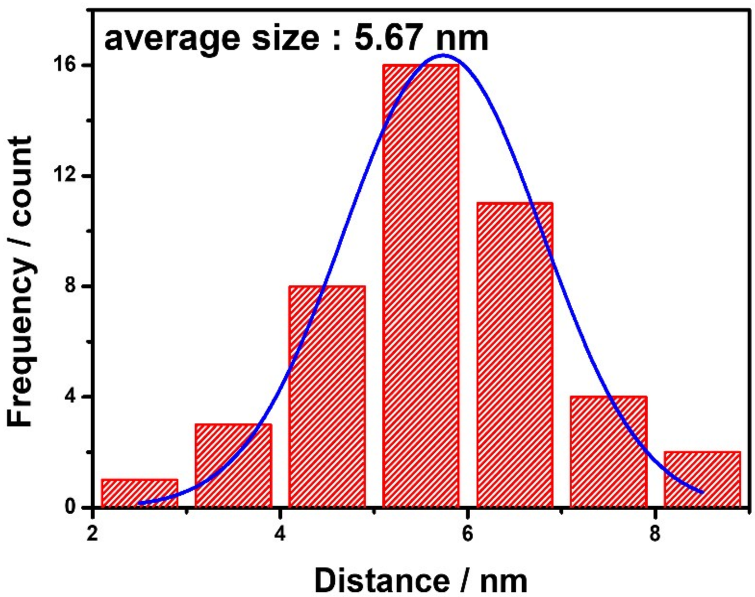

Fig. S4. Average particle size of Ni_2W_3N/NF.

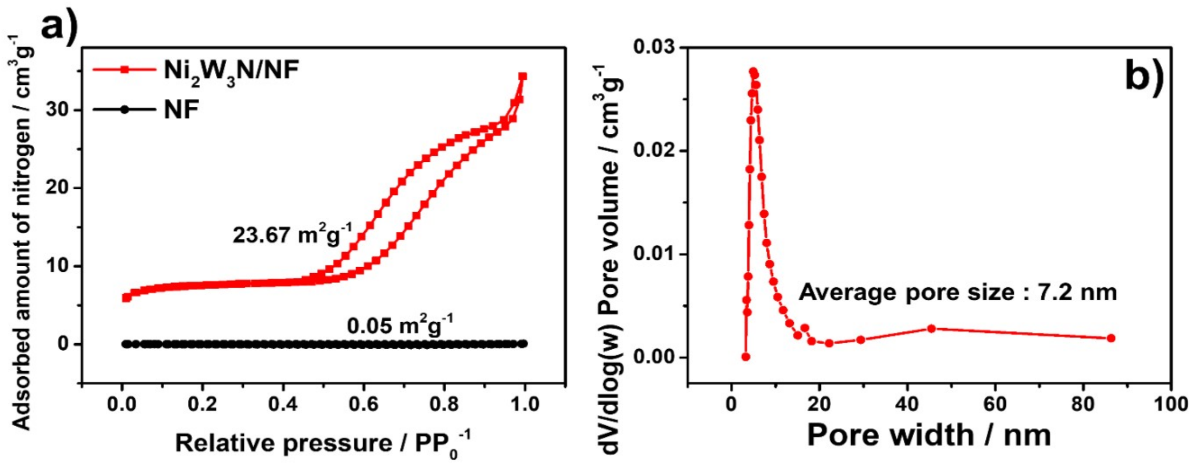

Fig. S5. (a) N_2 adsorption-desorption isotherms for Ni_2W_3N/NF and NF, (b) pore size distribution of Ni_2W_3N/NF.

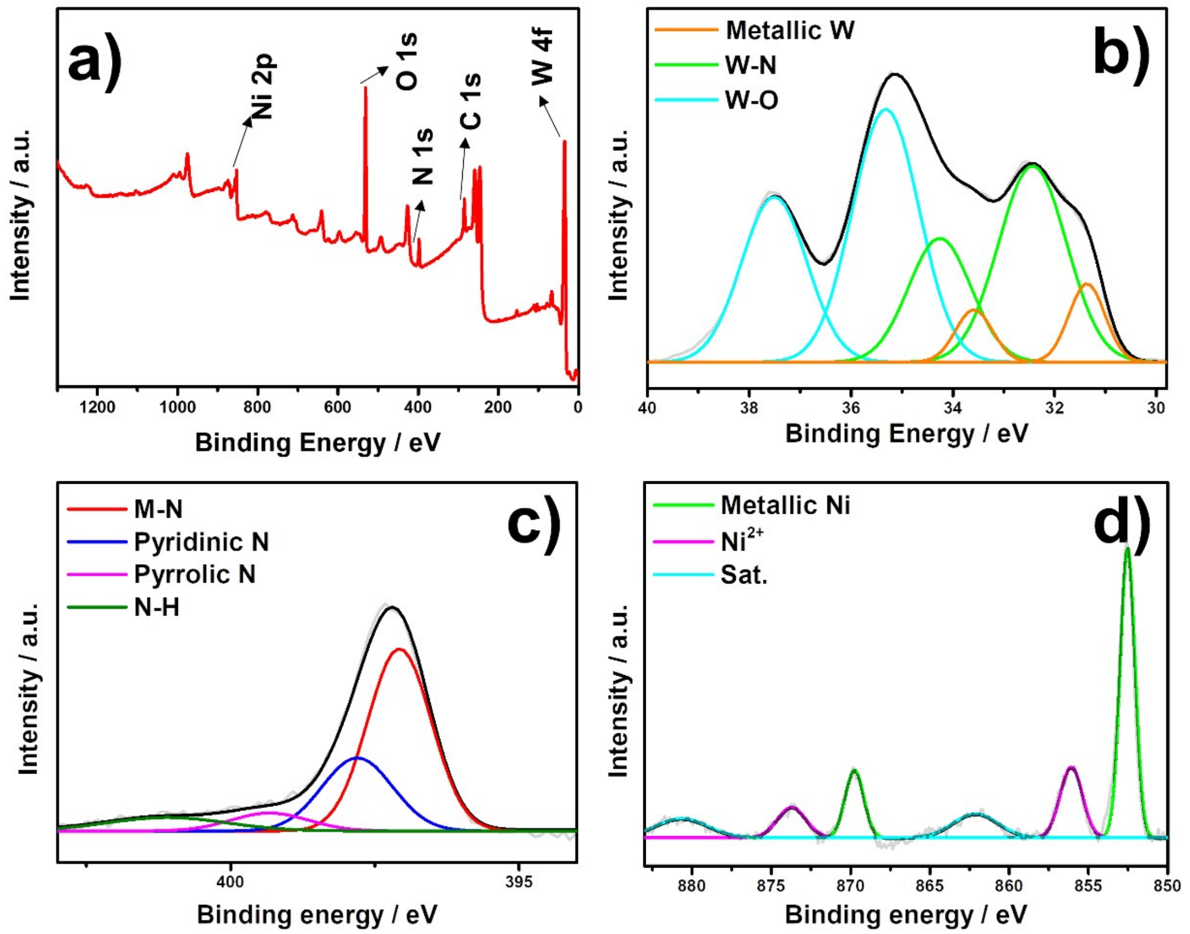

Fig. S6. XPS spectra of Ni_2W_3N/NF for (a) survey, (b) W 4f, (c) N 1s, and (d) Ni 2p.

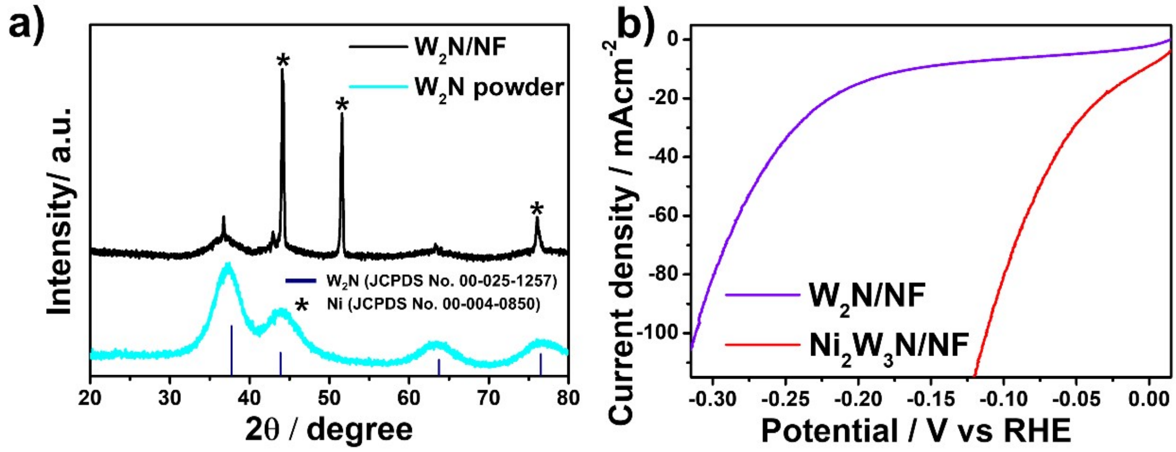

Fig. S7. (a) XRD patterns of W_2N powder and W_2N/NF. (b) The LSV curves of Ni_2W_3N/NF and W_2N/NF.

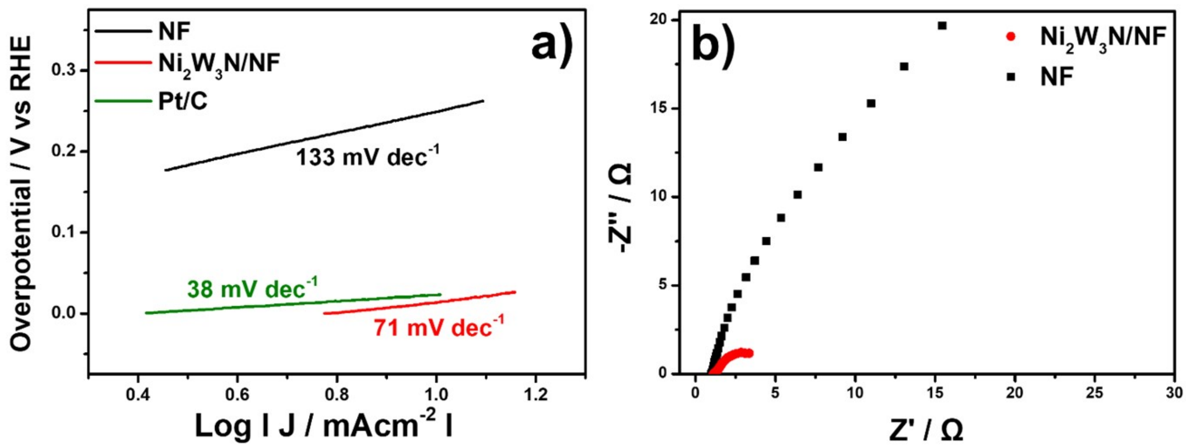

Fig. S8. (a) Tafel plots of Ni_2W_3N/NF, Pt/C, and NF. (b) Nyquist plots of Ni_2W_3N/NF and NF.

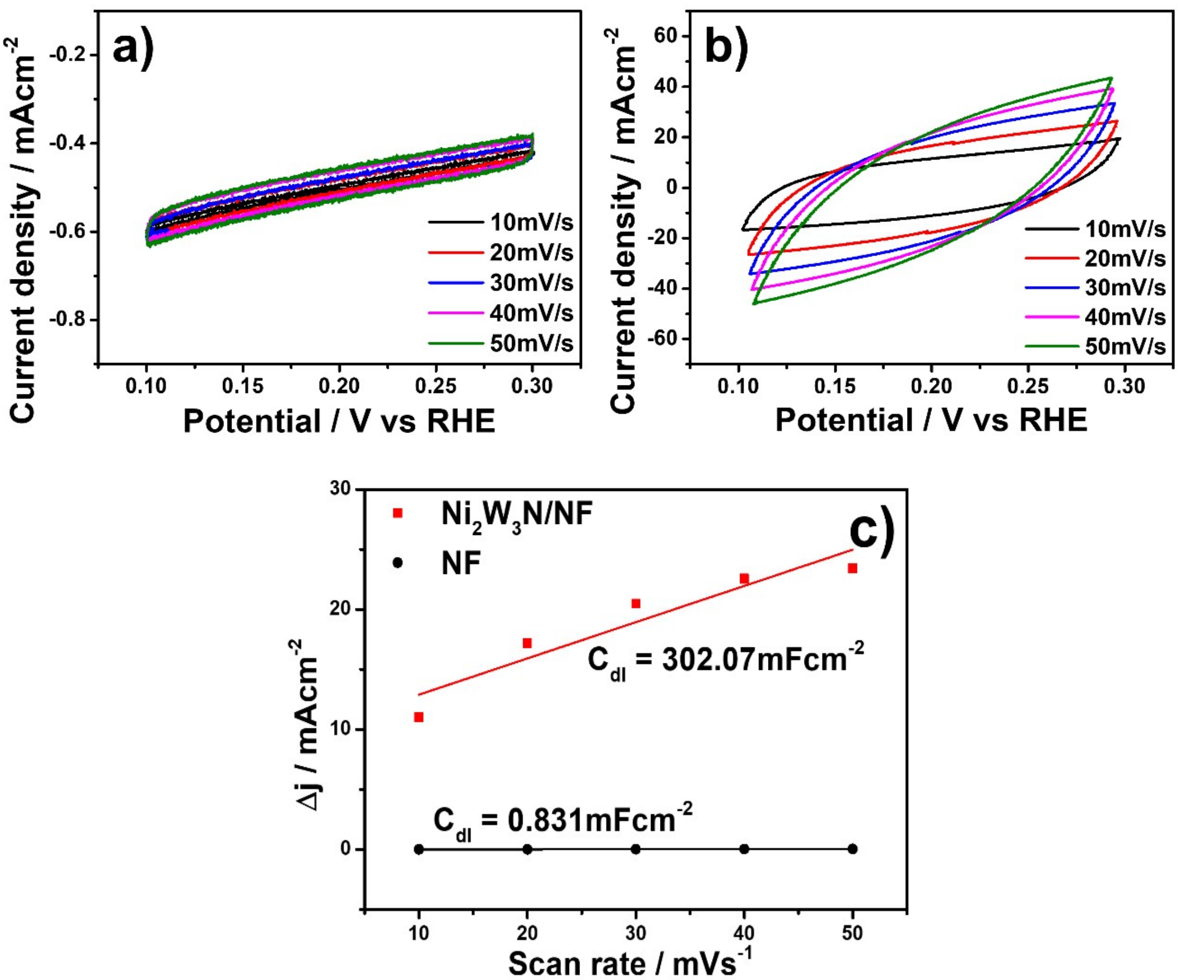

Fig. S9. Cyclic voltammograms of (a) NF and (b) Ni_2W_3N/NF at different scan rates. (c) measured capacitive current as a function of scan rate of Ni_2W_3N/NF, and NF.

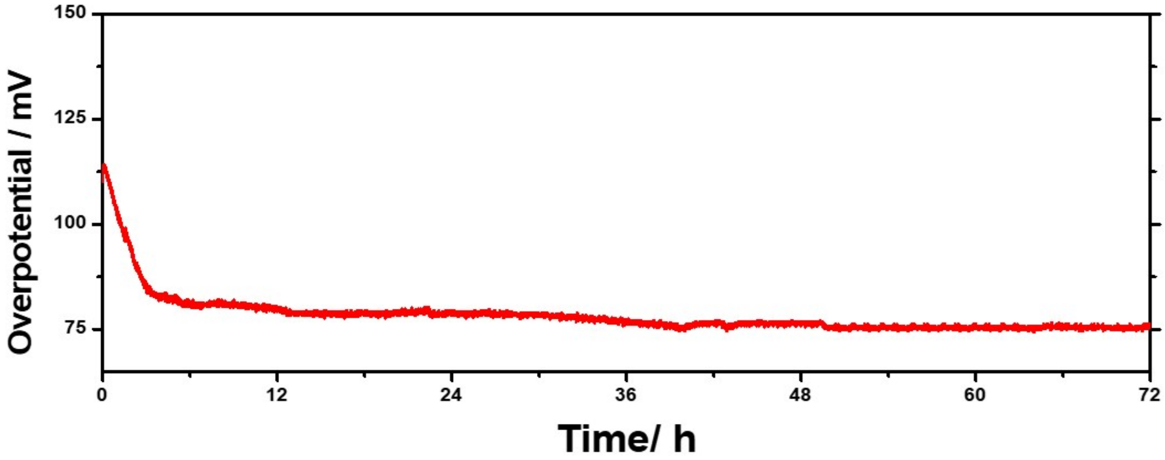

Fig. S10. Chronopotentiometric curve of Ni_2W_3N/NF at 100 mA cm^{-2} for 72 h.

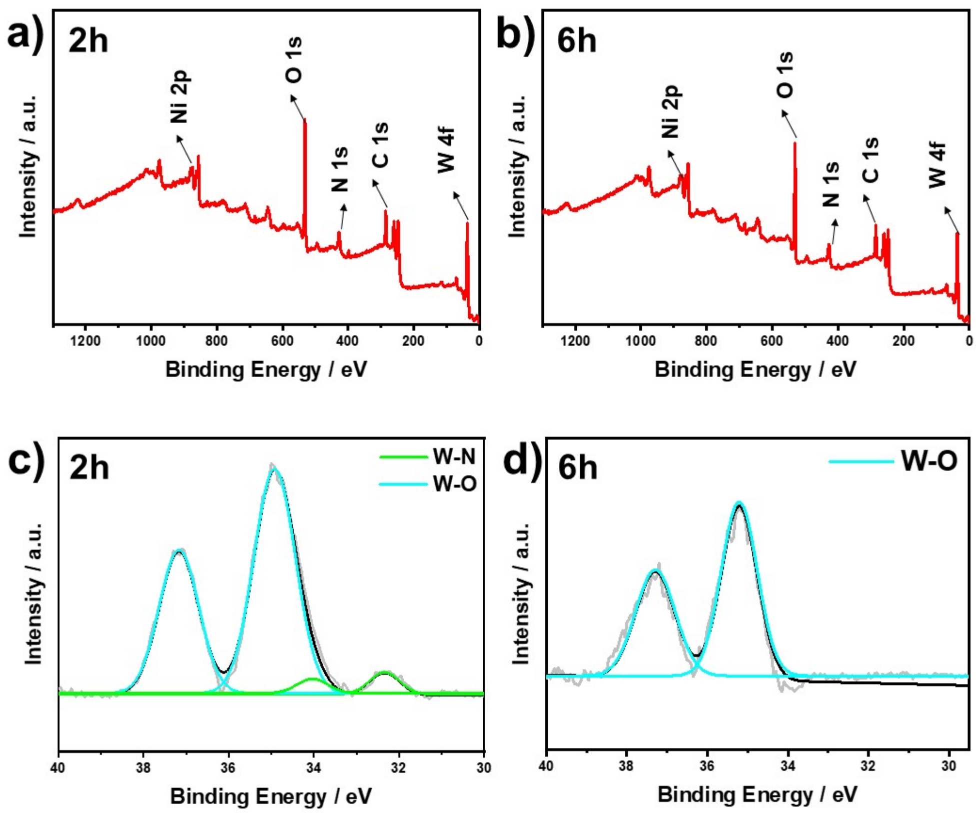

Fig. S11. XPS spectra of Ni_2W_3N/NF during the stability test (a) survey scan for 2h, (b) survey scan for 6h, (c) W 4f for 2h, and (d) W 4f for 6h.

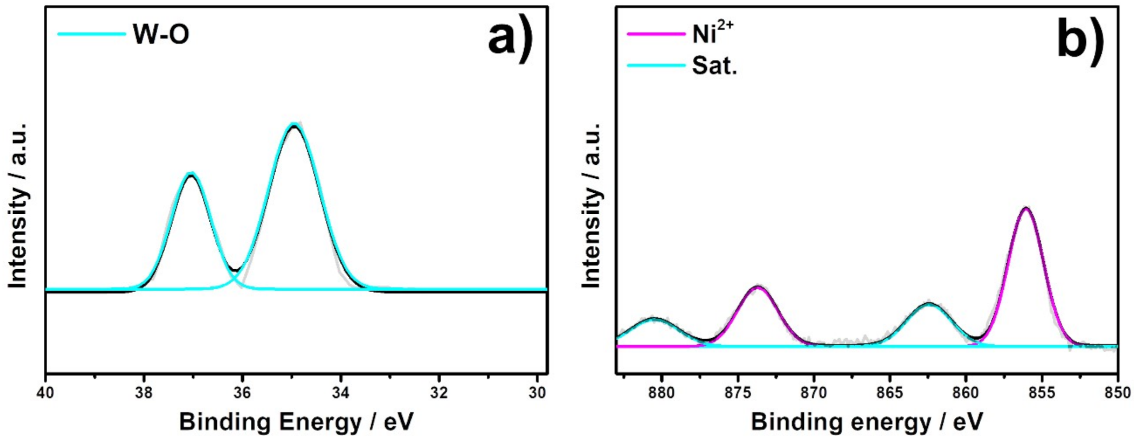

Fig. S12. XPS Spectra of after CP for 30 h of Ni_2W_3N/NF for (a) W 4f, (b) Ni 2p.

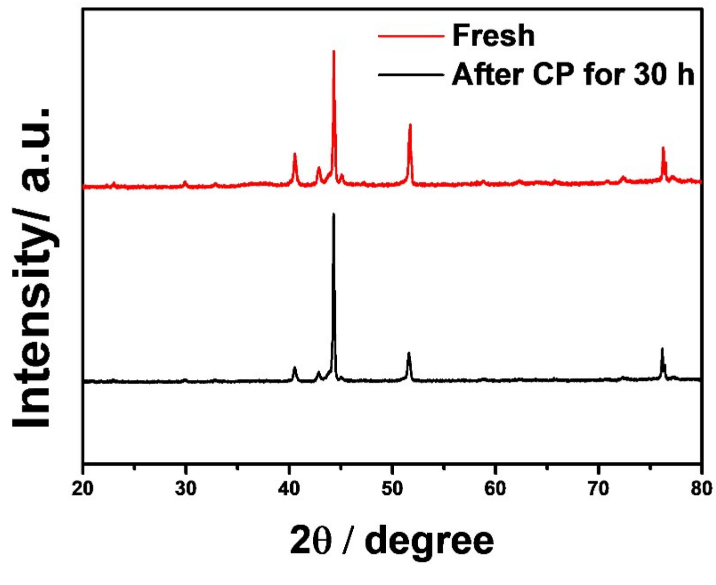

Fig. S13. XRD patterns of before and after CP for 30 h of Ni_2W_3N/NF.

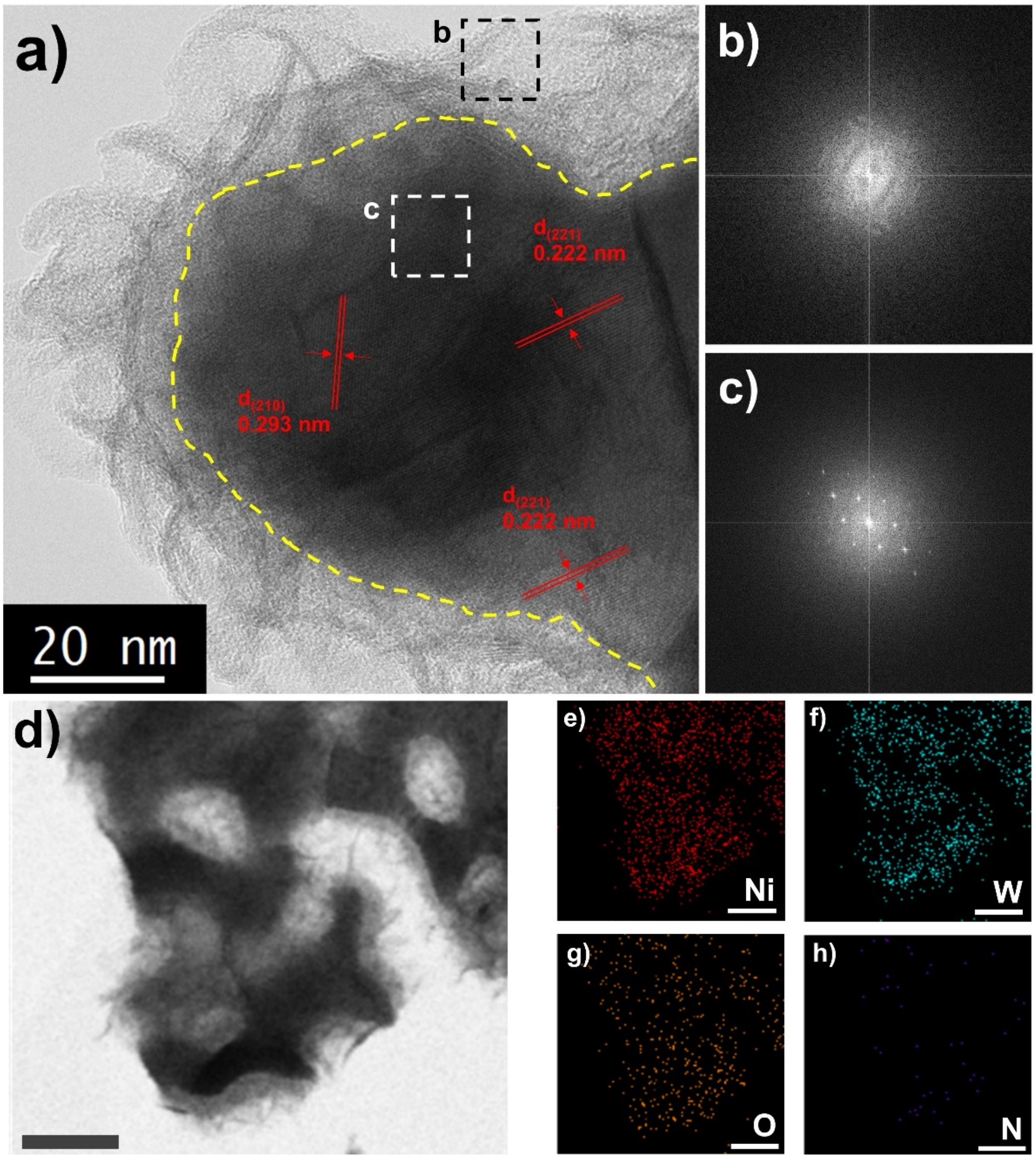

Fig. S14. (a) TEM image, (b), (c) FFT images, (d) HRTEM image (e) Ni, (f) W, (g) O, and (h) N.

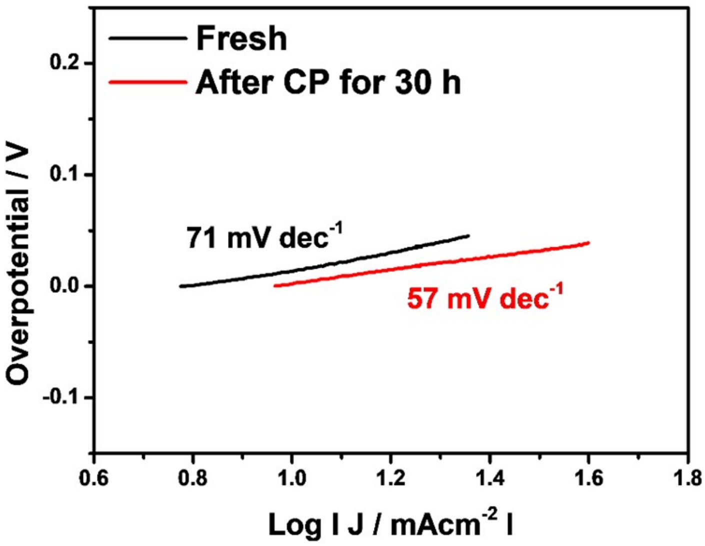

Fig. S15. Tafel plots of before and after CP for 30 h of Ni_2W_3N/NF.

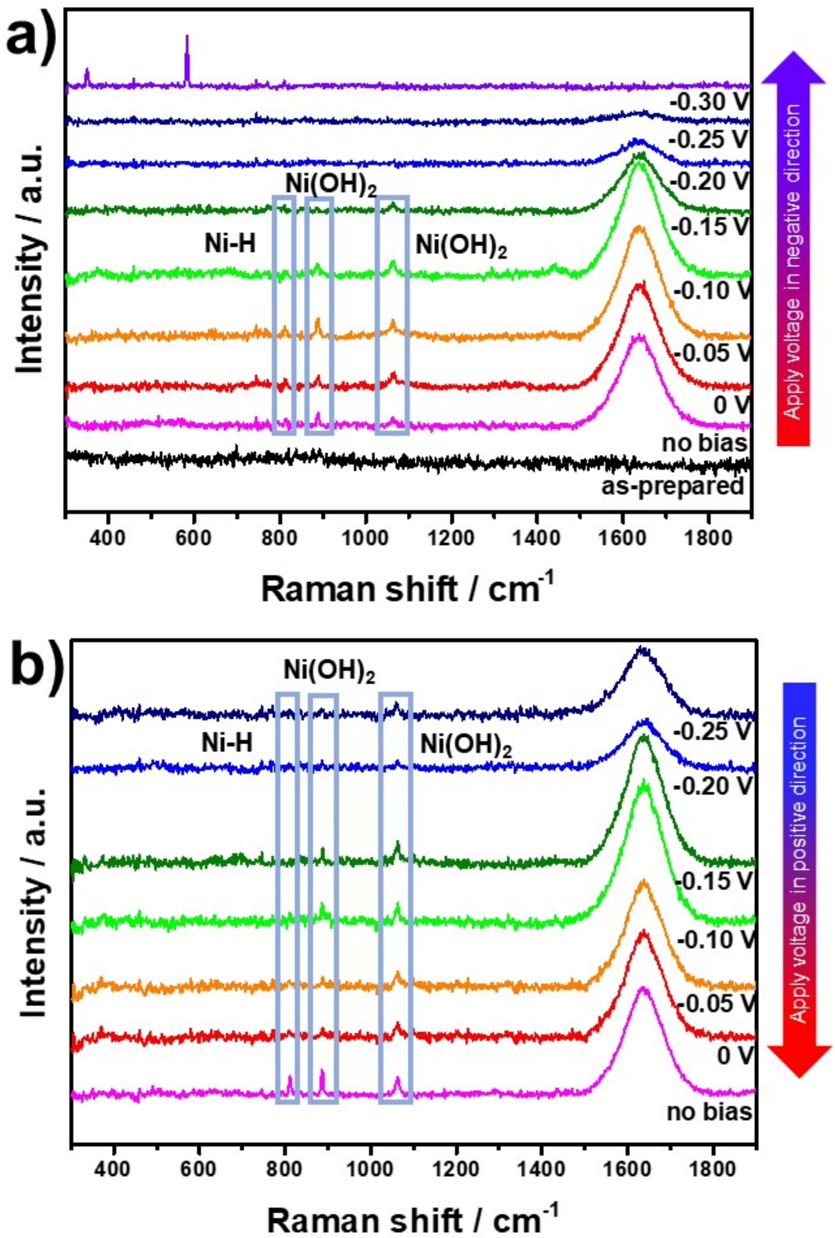

Fig. S16. Potential-dependent *in situ* Raman spectra of NF in 1 M KOH (a) applying voltage in the negative direction, and (b) applying voltage in the positive direction.

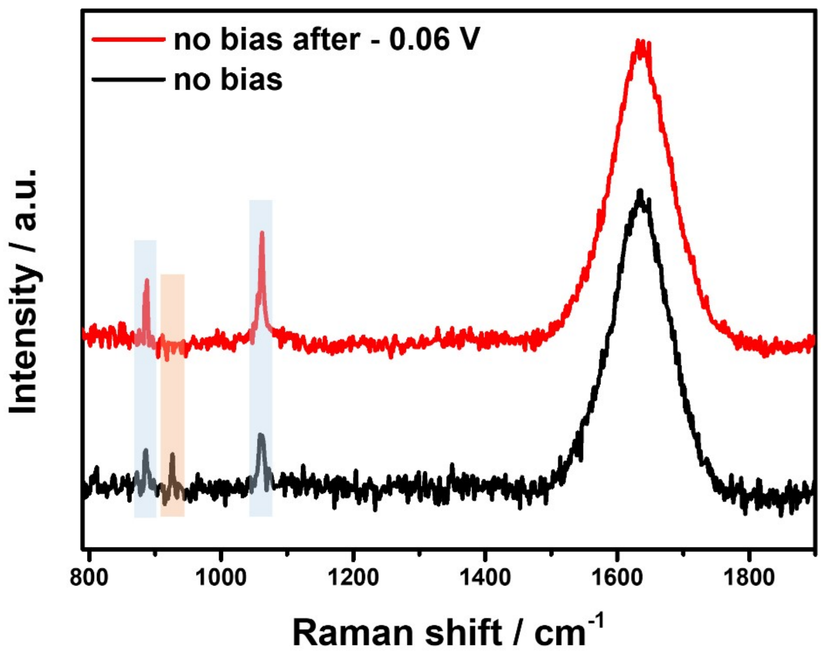

Fig. S17. The *ex-situ* Raman spectra of the no bias and after HER at -0.06 V of Ni_2W_3N/NF.

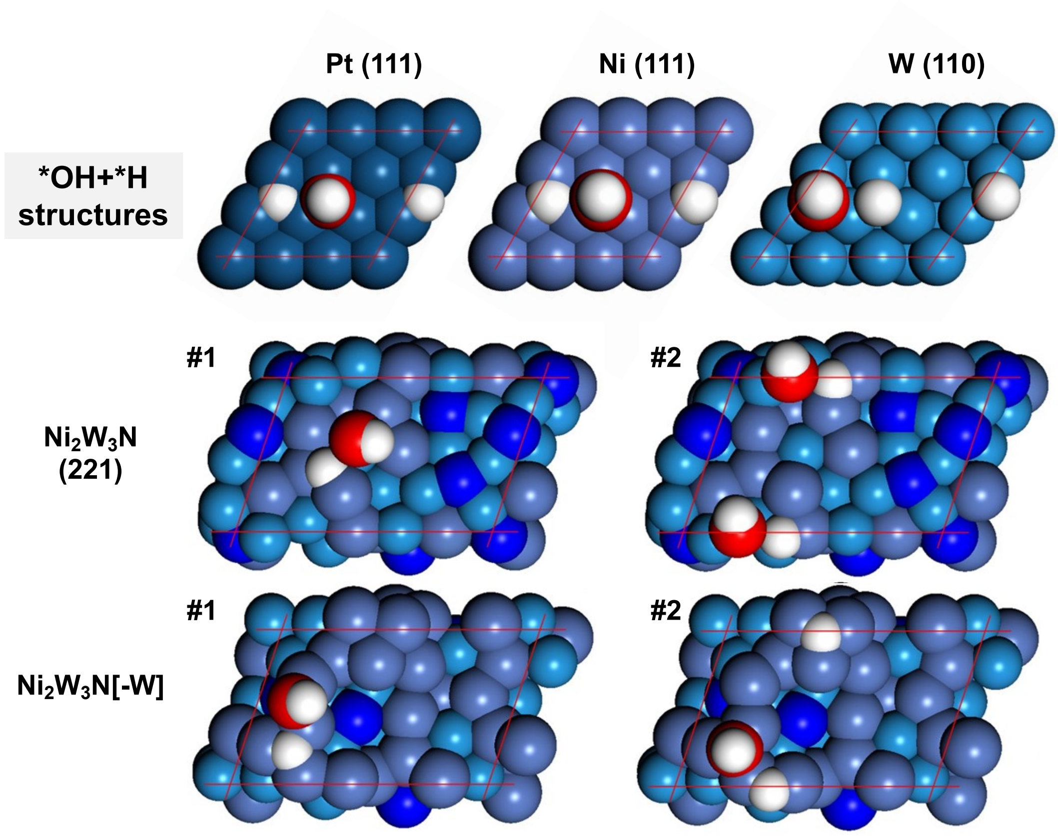

Fig. S18. Water dissociation structures on pure metal (Pt, Ni, W) and Ni_2W_3N surfaces.

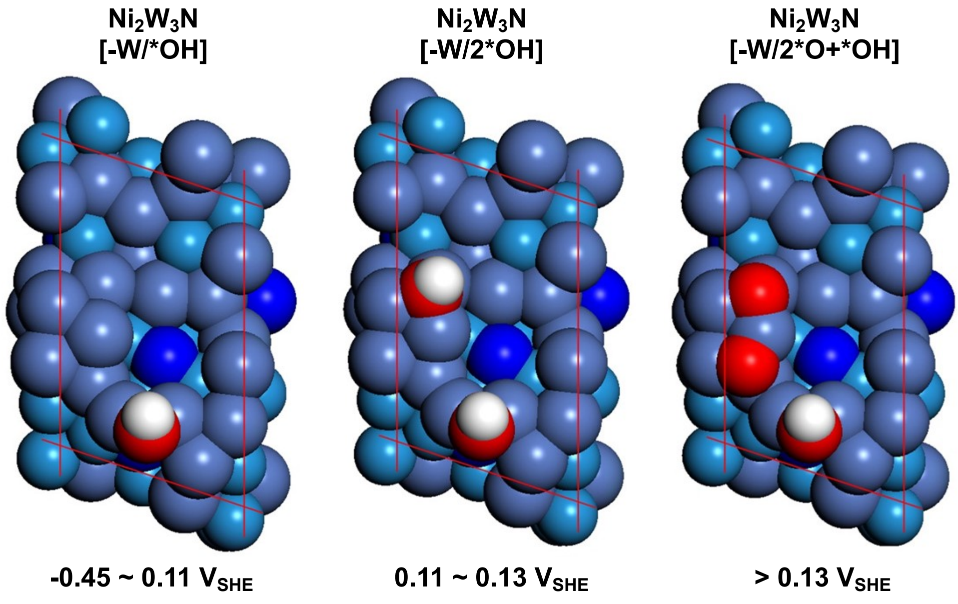

Fig. S19. The most stable surface functional groups on Ni_2W_3N[-W] as a function of electrochemical potential.

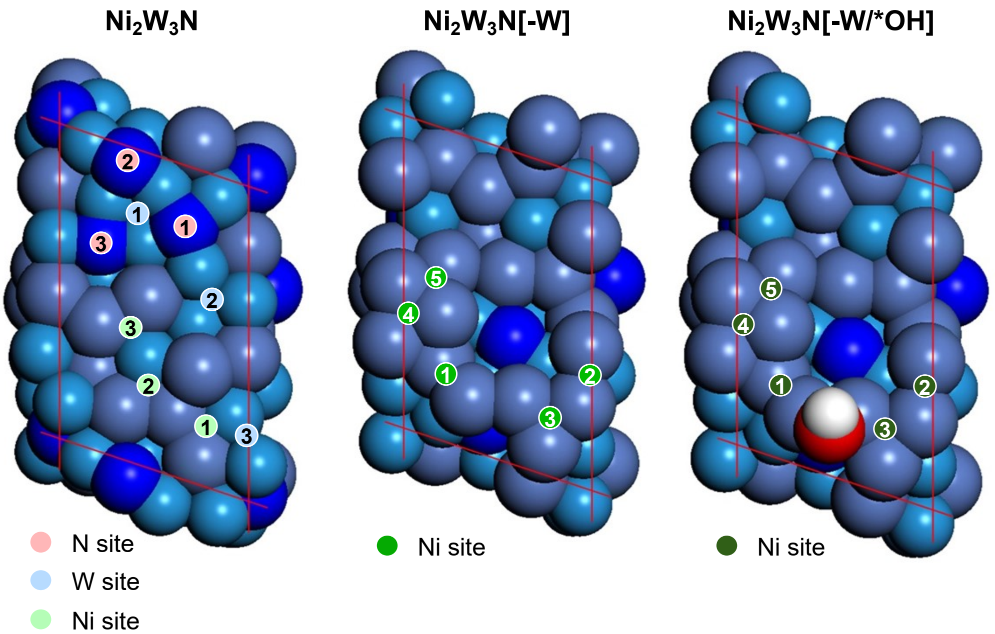

Fig. S20. Possible hydrogen binding sites for original Ni_2W_3N(221), W-leached Ni_2W_3N[-W], and *OH-attached Ni_2W_3N[-W/*OH] surfaces.

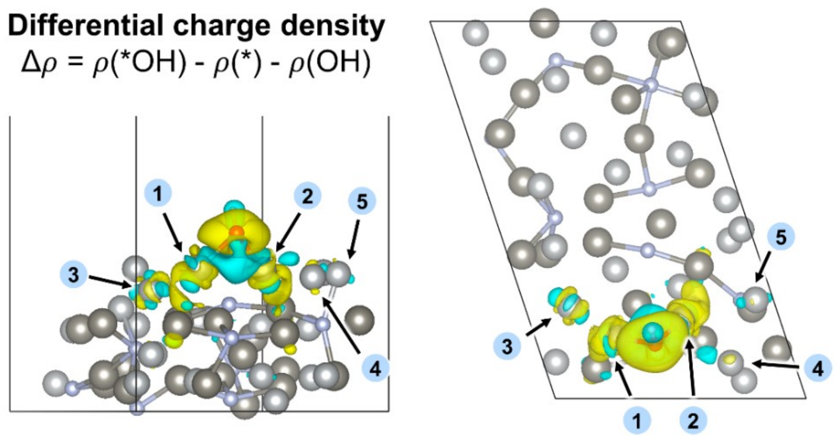

Bader partial charge @ Ni (*e*)

#	*	*OH
1	-0.17	+0.07
2	-0.21	+0.05
3	-0.18	-0.18
4	-0.23	-0.20
5	+0.06	+0.05

Fig. S21. Differential charge density iso-surface map of Ni_2W_3N[-W/*OH] surface and corresponding Bader partial charge analysis results. Adjacent Ni atoms (1 and 2) show significant electron depletion due to the electron-withdrawing effect of *OH.

Table S1. Comparison of the HER performance in alkaline media with reported bimetallic TMN-based catalysts.

	electrolyte	η_{50} [mV]	η_{100} [mV]	Tafel slope [mV dec $^{-1}$]	Reference
Ni_2W_3N/NF (Fresh)	1 M KOH	75.5	112	71	This work
Ni_2W_3N/NF (After CP for 30h)	1 M KOH	46.5	78.7	57	This work
Co_3Mo_3N/ Ni_3Mo_3N	1 M KOH	36 (η_{10})	130	53	[1]
Ni_3FeN@C/NF	1 M KOH	~200	277	131	[2]
NiMoN	1 M KOH	227	293	174	[3]
Co-Mo-N/NF	1 M KOH	81 (η_{10})	198	121	[4]
Ni_3Mo_3N-NC/NF	1 M KOH	39 (η_{10})	149	71	[5]
$NiMo_{0.75}N$/PNCT	1 M KOH	52 (η_{10})	~200	82	[6]
Co_2Ni_1N	1 M KOH	~200	N/A	60.17	[7]
Ni_2Mo_3N/NF	1 M KOH	89	123.8	62	[8]
$FeNi_3N$/NG	1 M KOH	98 (η_{20})	186	83.1	[9]
NiMoN-550	1 M KOH	159 (η_{20})	265	79	[10]
$CoMoN_x$-400 NSAs/NF	1 M KOH	91 (η_{10})	208	70.3	[11]
$Co_{3.2}Fe_{0.8}N$/NMC-100	1 M KOH	315 (η_{10})	N/A	N/A	[12]
$NiCo_2N$/NF	1 M KOH	~180 (η_{10})	N/A	79	[13]
$NiTiN_x$	1 M KOH	125 (η_{10})	~200	71	[14]
Ni_2Fe_2N/Ni_3Fe	1 M KOH	74 (η_{10})	N/A	53	[15]
V-Ni_2Mo_3N	1 M KOH	54 (η_{10})	117	42.8	[16]
MoVN	1 M KOH	108 (η_{10})	~180	60	[17]
$Cu_xNi_{4-x}N$/NF	1 M KOH	12 (η_{10})	111	86	[18]
Ni_3Mo_3N/NF-2.0	1 M KOH	28 (η_{10})	N/A	60	[19]
$Ni/Ni_{0.8}Mo_{4.2}N_6$	1 M KOH	20 (η_{10})	~130	38	[20]
Fe_2Ni_2N	1 M KOH	110 (η_{10})	~310	101	[21]

References

1. J. Tang, S. Zhang, Y. Zeng, B. Yang, K. Zhang, Y. Li, Y. Yao and J. Hu, *Chem. Eng. J.*, 2024, **487**, 150439.
2. B. Wang, M. Lu, D. Chen, Q. Zhang, W. Wang, Y. Kang, Z. Fang, G. Pang and S. Feng, *J. Mater. Chem. A*, 2021, **9**, 13562-13569.
3. V. Jayaraman, G. Jang, G.-H. Noh, M. Murmu and D.-H. Kim, *J. Mater. Chem. A*, 2024., doi: https://doi.org/10.1039/D4TA01117A
4. J. Zhu, Q. Du, M. A. Khan, H. Zhao, J. Fang, D. Ye and J. Zhang, *Appl. Surf. Sci.*, 2023, **623**, 156989.
5. P. Tan, Y. Wang, L. Yang, X. Zhang and J. Pan, *Diam. Relat. Mater.*, 2023, **136**, 109974.
6. B. Jiang, J. Li, Y. Cui, S. Shi, N. Jiang and J. Guan, *J. Alloys Compd.*, 2023, **958**, 170371.
7. X. Feng, H. Wang, X. Bo and L. Guo, *ACS Appl. Mater. Interfaces*, 2019, **11**, 8018-8024.
8. S. H. Park, T. H. Jo, M. H. Lee, K. Kawashima, C. B. Mullins, H.-K. Lim and D. H. Youn, *J. Mater. Chem. A*, 2021, **9**, 4945-4951.
9. L. Liu, F. Yan, K. Li, C. Zhu, Y. Xie, X. Zhang and Y. Chen, *J. Mater. Chem. A*, 2019, **7**, 1083-1091.
10. Z. Yin, Y. Sun, C. Zhu, C. Li, X. Zhang and Y. Chen, *J. Mater. Chem. A*, 2017, **5**, 13648-13658.
11. Y. Lu, Z. Li, Y. Xu, L. Tang, S. Xu, D. Li, J. Zhu and D. Jiang, *Chem. Eng. J*, 2021, **411**, 128433.
12. K. Zhang, W. Mai, J. Li, G. Li, L. Tian and W. Hu, *ACS Appl. Nano Mater.*, 2019, **2**, 5931-5941.
13. Y. Wang, B. Zhang, W. Pan, H. Ma and J. Zhang, *ChemSusChem*, 2017, **10**, 4170-4177.
14. S. Tang, B. Ouyang, H. Tan, W. Zhou, Z. Ma and Y. Zhang, *Electrochim. Acta*, 2020, **362**, 137222.
15. Y. Hu, T. Xiong, M.-S. J. T. Balogun, Y. Huang, D. Adekoya, S. Zhang and Y. Tong, *Mater. Today Phys.*, 2020, **15**, 100267.
16. P. Zhou, X. Lv, Y. Gao, Z. Liang, Y. Liu, Z. Wang, P. Wang, Z. Zheng, Y. Dai and B. Huang, *Electrochim. Acta*, 2020, **337**, 135689.
17. B. Wei, G. Tang, H. Liang, Z. Qi, D. Zhang, W. Hu, H. Shen and Z. Wang, *Electrochem. Commun.*, 2018, **93**, 166-170.
18. Y. Ma, Z. He, Z. Wu, B. Zhang, Y. Zhang, S. Ding and C. Xiao, *J Mater. Chem. A*, 2017, **5**, 24850-24858.
19. Q. Zhang, H. Zhang, C. Lin, Z. Zhang, X. Zuo, Q. Yang, H. Tang and G. Li, *J. Electrochem. Soc.*, 2024, **171**, 053511.
20. S. Liang, H. Hu, J. Liu, H. Shen, Q. Li, N. Qiu, H. Guo, X. Guo, S. Du and Y. Zhu, *Appl. Catal. B: Environ.*, 2023, **337**, 123008.
21. M. Jiang, Y. Li, Z. Lu, X. Sun and X. Duan, *Inorg. Chem. Front.*, 2016, **3**, 630-634.